View metadata, citation and similar papers at core.ac.uk

brought to you by CORE

provided by IUPUIScholarWorks

Facile synthesis of carbon-11-labeled sEH/PDE4 dual inhibitors as new potential PET agents for imaging of sEH/PDE4 enzymes in neuroinflammation

Limeng Jia[a], Caihong Miao[a], Fugui Dong[a], Wei Li[a], Min Wang[b], Qi-Huang Zheng[b,*], Zhidong Xu[a,c,d*]

[a]*Key Laboratory of Medicinal Chemistry and Molecular Diagnosis of Ministry of Education, College of Chemistry and Environmental Science, Hebei University, Baoding, Hebei 071002, China*

[b]*Department of Radiology and Imaging Sciences, Indiana University School of Medicine, 1345 West 16th Street, Room 202, Indianapolis, IN 46202, USA*

[c]*College of Chemical & Pharmaceutical Engineering, Key Laboratory of Molecular Chemistry for Medicine of Hebei Province, Hebei University of Science & Technology, Shijiazhuang, Hebei 050018, China*

[d]*Shijiazhuang Vince Pharmatech Co., Ltd., Shijiazhuang, Hebei 050030, China*

*Corresponding authors. E-mail address: qzheng@iupui.edu (Q.-H. Zheng); zhidongxu@hbu.edu.cn (Z. Xu).

This is where the receipt/accepted dates will go; Received Month XX, 2019; Accepted Month XX, 2019 [BMCL RECEIPT]

Abstract—To develop PET tracers for imaging of neuroinflammation, new carbon-11-labeled sEH/PDE4 dual inhibitors have been synthesized. The reference standard *N*-(4-methoxy-2-(trifluoromethyl)benzyl)benzamide (**1**) and its corresponding desmethylated precursor *N*-(4-hydroxy-2-(trifluoromethyl)benzyl)benzamide (**2**) were synthesized from (4-methoxy-2-(trifluoromethyl)phenyl)methanamine and benzoic acid in one and two steps with 84% and 49% overall chemical yield, respectively. The standard *N*-(4-methoxy-2-(trifluoromethyl)benzyl)-1-propionylpiperidine-4-carboxamide (MPPA, **4**) and its precursor *N*-(4-hydroxy-2-(trifluoromethyl)benzyl)-1-propionylpiperidine-4-carboxamide (**5**) were synthesized from methyl 4-piperidinecarboxylate, propionyl chloride and (4-methoxy-2-(trifluoromethyl)phenyl)methanamine in two and three steps with 62% and 34% overall chemical yield, respectively. The target tracers *N*-(4-[^{11}C]methoxy-2-(trifluoromethyl)benzyl)benzamide ([^{11}C]**1**) and *N*-(4-[^{11}C]methoxy-2-(trifluoromethyl)benzyl)-1-propionylpiperidine-4-carboxamide ([^{11}C]MPPA, [^{11}C]**4**) were prepared from their corresponding precursors **2** and **5** with [^{11}C]CH_3OTf through *O*-[^{11}C]methylation and isolated by HPLC combined with SPE in 25-35% radiochemical yield, based on [^{11}C]CO_2 and decay corrected to end of bombardment (EOB). The radiochemical purity was >99%, and the molar activity (A_M) at EOB was 370-740 GBq/μmol with a total synthesis time of 35-40-minutes from EOB.

Keywords: Soluble epoxide hydrolase (sEH); Phosphodiesterase 4 (PDE4); Carbon-11-labeled sEH/PDE4 dual inhibitors; Radiosynthesis; Positron emission tomography (PET); Neuroinflammation.

Inflammation is a complex biological process and part of the body's immune response involving immune cells, blood vessels, and molecular mediators for self-protection to remove harmful stimuli, including damaged cells, irritants, or pathogens.[1] Neuroinflammation is the inflammation of the nervous tissue, and it is associated with central nervous system (CNS) diseases including Alzheimer's disease (AD), Parkinson's disease (PD), Huntington's disease (HD), multiple sclerosis (MS), amyotrophic lateral sclerosis (ALS), traumatic brain injury (TBI) and stroke.[1-4] Molecular imaging of neuroinflammation in

---

This is the author's manuscript of the article published in final edited form as:

Jia, L., Miao, C., Dong, F., Li, W., Wang, M., Zheng, Q.-H., & Xu, Z. (2019). Facile synthesis of carbon-11-labeled sEH/PDE4 dual inhibitors as new potential PET agents for imaging of sEH/PDE4 enzymes in neuroinflammation. Bioorganic & Medicinal Chemistry Letters, 29(13), 1654–1659. https://doi.org/10.1016/j.bmcl.2019.04.036

neurodegenerative diseases by positron emission tomography (PET) is one of the most active as well as most challenging areas in neuroscience, because PET neuroimaging can offer various non- or minimally invasive techniques to characterize neuroinflammatory processes for the purpose of diagnosis, therapy and treatment monitoring.[5-8] Many enzyme- or receptor-based radioligands have been developed for *in vivo* PET visualization of neuroinflammation.[9-11] We are interested in the development of new PET radioligands for neuroinflammation. In our previous work, we have synthesized and developed a series of PET radiotracers[12-20] that target the enzyme or receptor for neuroinflammation such as [^{11}C]FMAME for matrix metalloproteinase (MMP), carbon-11-labeled celecoxib derivatives for cyclooxygenase-2 (COX-2), [^{11}C]PBR28 for translocator protein (TSPO), [^{11}C]MCFA for cannabinoid receptor 2 (CB2), [^{11}C] SB-216763 for glycogen synthase kinase 3 (GSK-3), [^{11}C]MABL for CX_3C chemokine receptor 1 (CX_3CR1), [^{11}C]GSK1482160 for purinergic receptor ($P2X_7$) and [^{11}C]MMPC for interleukin-1 receptor-associated kinase 4 (IRAK4), as indicated in **Figure 1**. Traditionally drugs including PET drugs have been designed based on single-target approach, however, in complex diseases where single-target drugs have failed or show severe limitations, multi-target drugs have emerged as more effective therapeutic approach, since drug molecules often interact with multiple targets.[21-24] Subsequently, PET radioligand design has benefited from the multi-target approach in drug design and discovery, which opens new avenues to rationally develop next generation of more effective PET agents. In this ongoing study, we first select the dual enzymes soluble epoxide hydrolase (sEH)/phosphodiesterase 4 (PDE4) as another more specific neuroinflammatory target for PET imaging. Both sEH and PDE4 are critical enzymes in neuroinflammation and play an important role in the progression of various neurodegenerative diseases including AD.[25] Small drug molecules targeting on multiple proteins have attracted tremendous interest for developing therapeutics, and dual sEH/PDE4 inhibitors for the treatment of inflammatory diseases represent this multi-target therapeutic strategy. To improve the treatment of complex diseases, multitarget ligands have been designed and developed.[26] Recently, bioavailable sEH/PDE4 dual inhibitors have been developed to treat inflammatory pain, the representative compound *N*-(4-methoxy-2-(trifluoromethyl)benzyl)-1-propionylpiperidine-4-carboxamide (MPPA, **4**) displayed good efficacy in *in vitro* assays with IC_{50} 2.1 nM (hsEH) and 8.1 nM (PDE4), and a derivative *N*-(4-methoxy-2-(trifluoromethyl)benzyl)benzamide (**1**) exhibited similar *in vitro* efficacy with IC_{50} 2 nM (hsEH).[25] Radiolabeled PDE4 inhibitors such as [^{11}C]*R*-(-)-Rolipram (**Figure 1**) have been developed and evaluated in animal and human PET studies.[27] Likewise, radiolabeled sEH inhibitors like [^{18}F]FNDP (**Figure 1**) have been developed and evaluated in animals.[28] However, the PubMed search showed no records on radiolabeled sEH/PDE4 dual inhibitors. It is clear PET imaging modality can accurately measure the protein expression in biological process and diseases, but it will be still challenging to assess the changes of dual proteins expression level using dual proteins target radiotracers. The key point is that a sEH/PDE4 dual inhibitor should have favorable *in vitro* biological activity for both protein targets first. Here we report the design, synthesis and labeling of radiolabeled sEH/PDE4 dual inhibitors, *N*-(4-[^{11}C]methoxy-2-(trifluoromethyl)benzyl)benzamide ([^{11}C]**1**) and *N*-(4-[^{11}C]methoxy-2-(trifluoromethyl)benzyl)-1-propionylpiperidine-4-carboxamide ([^{11}C]MPPA, [^{11}C]**4**) (**Figure 1**), as new candidate PET neuroinflammation imaging agents, for the first time.

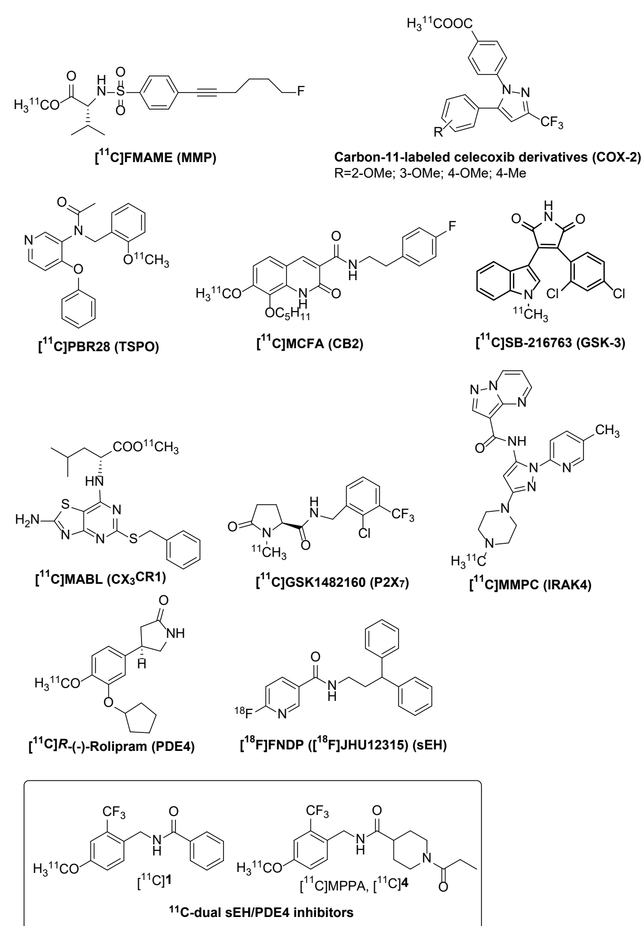

Figure 1. PET radiotracers for imaging of neuroinflammation.

IC_{50} values for [^{11}C]MPPA are 2.1 nM (hsEH) and 8.1 nM (PDE4),[25] compared to previously reported [^{18}F]FNDP (IC_{50} 8.66 nM for sEH)[28] and [^{11}C]*R*-(-)-Rolipram (IC_{50} 290 nM for PDE4),[29] the results suggest the imaging probes developed in this study have

superior *in vitro* biological data to [^{11}C]*R*-(-)-Rolipram and [^{18}F]FNDP.

Synthesis of the reference standards **1**, **4**; and their corresponding desmethylated precursors *N*-(4-hydroxy-2-(trifluoromethyl)benzyl)benzamide (**2**), *N*-(4-hydroxy-2-(trifluoromethyl)benzyl)-1-propionylpiperidine-4-carboxamide (**5**) is depicted in **Scheme 1**, according to the reported procedures.[25,30-34] Compounds **1** and **4** were prepared by an amidation reaction from commercially procured (4-methoxy-2-(trifluoromethyl)phenyl)methanamine and benzoic acid or propionylpiperidine-4-carboxylic acid (**3**) in the presence of 1-ethyl-3-(3-(dimethylamino)-propyl)carbodiimide (EDC) and 4-(dimethylamino)-pyridine (DMAP) in 84% and 70% yield, respectively. Compound **3** was prepared from 4-piperidinecarboxylate through an amidation reaction with propionyl chloride, and then hydrolyzed with aqueous NaOH in 88% yield. The desmethylated precursors **2** and **5** were obtained by desmethylation reaction of the reference standards **1** and **4** with BBr_3 in CH_2Cl_2 at 0 ºC in 59% and 55% yield, respectively.

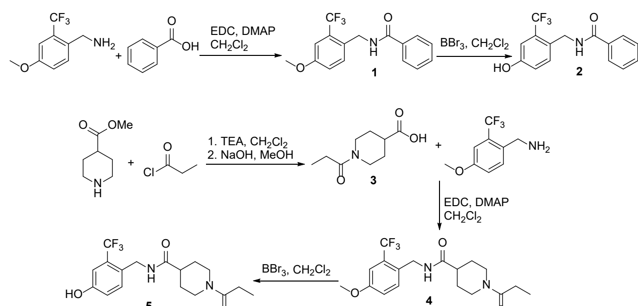

Scheme 1. Synthesis of reference standards **1**, **4** and precursors **2**, **5**.

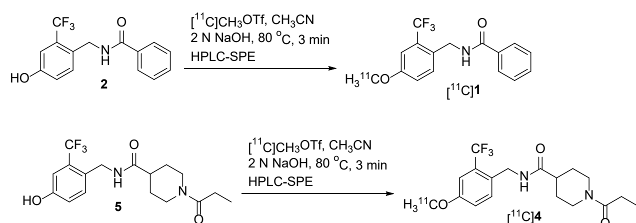

Scheme 2. Synthesis of target tracers [^{11}C]**1** and [^{11}C]**4**.

Synthesis of the target tracers [^{11}C]**1** and [^{11}C]**4** is presented in **Scheme 2**. The desmethylated precursor **2** or **5** underwent *O*-[^{11}C]methylation[35] using the reactive [^{11}C]methylating agent [^{11}C]methyl triflate ([^{11}C]CH_3OTf)[36,37] in acetonitrile at 80 °C under basic conditions (2 N NaOH). The product was isolated by semi-preparative reverse-phase (RP) high performance liquid chromatography (HPLC) with a C-18 column, and then concentrated by solid-phase extraction (SPE) with a disposable C-18 Plus Sep-Pak cartridge to produce the corresponding pure radiolabeled compound [^{11}C]**1** or [^{11}C]**4** in 25-35% radiochemical yield, decay corrected to end of bombardment (EOB), based on [^{11}C]CO_2.

The radiosynthesis was performed in a home-built automated multi-purpose [^{11}C]-radiosynthesis module.[38-40] Our radiosynthesis module facilitated the overall design of the reaction, purification and reformulation capabilities in a fashion suitable for adaptation to preparation of human doses. The radiosynthesis includes three stages: 1) labeling reaction; 2) purification; and 3) formulation. The overall synthesis time was 35-40 min from EOB. Our module is also designed to allow in-process measurement of [^{11}C]-tracer molar activity (A_M, GBq/μmol at EOB) using a radiation detector with a UV detector at the outlet of the HPLC-portion of the system. At the end of synthesis (EOS), the A_M of [^{11}C]-tracer was determined again by analytical RP-HPLC, calculated, decay corrected to EOB, and based on [^{11}C]CO_2, which was in agreement with the 'on line' determined value. The A_M of [^{11}C]**1** and [^{11}C]**4** produced in our PET chemistry facility was in the range of 370-740 GBq/μmol at EOB, using the Siemens RDS-111 Eclipse cyclotron ^{11}C-gas target, the Eckert & Ziegler Modular Lab C-11 Methyl Iodide/Triflate module, and our [^{11}C]-radiosynthesis unit.[35]

Chemical purity and radiochemical purity were determined by analytical RP-HPLC.[41] The chemical purity of the precursor and reference standard was >90% determined by RP-HPLC through UV flow detector. A representative analytical RP-HPLC chromatographic profile for the tracers [^{11}C]**1** and [^{11}C]**4**, Radio-HPLC (**A**) and UV-HPLC (**B**) traces for [^{11}C]**1**; Radio-HPLC (**C**) and UV-HPLC (**D**) traces for [^{11}C]**4**, is shown in **Figure 2**. The radiochemical purity of the target tracer [^{11}C]**1** or [^{11}C]**4** was >99% determined by Radio-HPLC through γ-ray (PIN diode) flow detector as indicated in **Figure 2**, **A** or **C**. The chemical purity of the target tracer [^{11}C]**1** or [^{11}C]**4** was simultaneously determined by UV-HPLC through UV flow detector as indicated in **Figure 2**, **B** or **D**. The minor impurities included its corresponding labeling precursor **2** or **5** and a few unknown UV peaks from the saline used in tracer formulation after HPLC-SPE purification. However, there is no chemical purity of the tracer release limit in PET tracer production, because the radiosynthesis is a micro-scale synthesis, and the radiotracer prepared is very trace amount.

The stability of the labeled tracers [^{11}C]**1** and [^{11}C]**4** was evaluated by analytical HPLC from EOS up to 3 h, one injection of the tracer solution in EtOH/saline onto HPLC column per hour. The HPLC chromatograms showed [^{11}C]**1** and [^{11}C]**4** were stable without decomposition.

A. Analytical radioactive HPLC trace for [^{11}C]**1**, Retention time (t_R) = 6.64 min

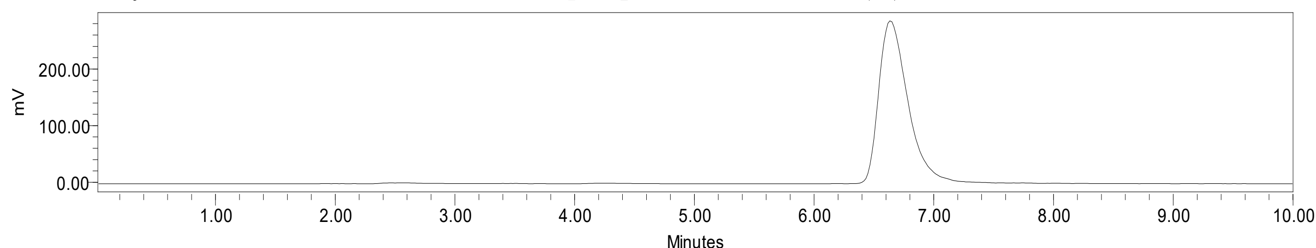

B. Analytical UV HPLC trace for [^{11}C]**1**, t_R = 6.56 min

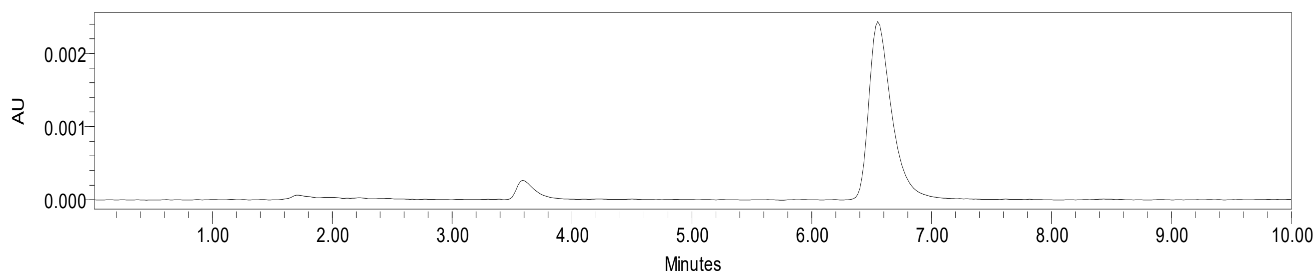

C. Analytical radioactive HPLC trace for [^{11}C]**4**, t_R = 4.31 min

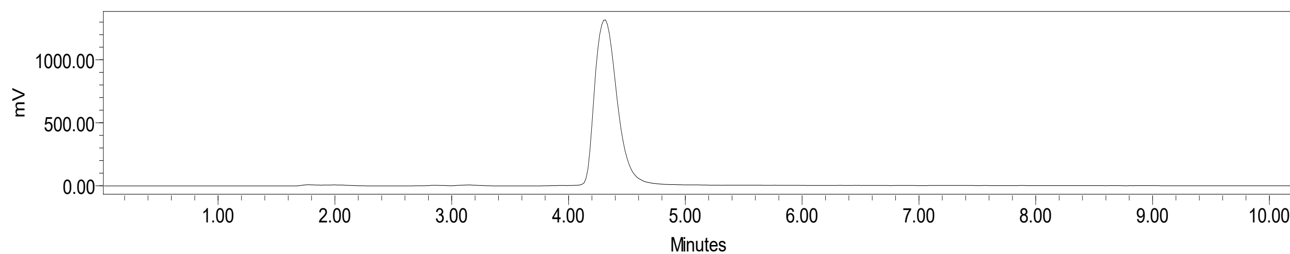

D. Analytical UV HPLC trace for [^{11}C]**4**, t_R = 4.23 min

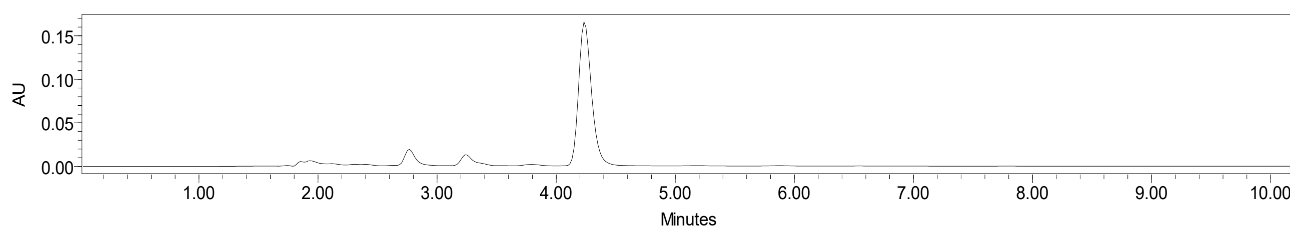

Figure 2. A representative analytical RP-HPLC chromatographic profile for the tracers [^{11}C]**1** and [^{11}C]**4**: (**A**) Radio-HPLC trace for [^{11}C]**1** and (**B**) UV-HPLC trace for [^{11}C]**1**; (**C**) Radio-HPLC trace for [^{11}C]**4** and (**D**) UV-HPLC trace for [^{11}C]**4**. Analytical RP-HPLC conditions were a Prodigy (Phenomenex) 5 μm C-18 column, 4.6 × 250 mm; mobile phase 65% CH_3CN/35% 4.0 mM CH_3COONa; flow rate 1.0 mL/min; UV (254 nm) and γ-ray (PIN diode) flow detectors.

The experimental details and characterization data for compounds **1-5** and for the tracers [^{11}C]**1** and [^{11}C]**4** are given.[42]

In summary, facile synthetic routes with moderate to high yields have been developed to produce the reference standards **1** and **4**, desmethylated precursors **2** and **5**, and target tracers [^{11}C]**1** and [^{11}C]**4**. The radiosynthesis employed [^{11}C]CH_3OTf for *O*-[^{11}C]methylation at the phenol hydroxyl position of the desmethylated precursor, followed by product purification and isolation using a semi-preparative RP HPLC combined with SPE. [^{11}C]**1** and [^{11}C]**4** were obtained in high radiochemical yield, radiochemical purity and chemical purity, with a reasonably short overall synthesis time, and high molar activity. This will facilitate studies to evaluate [^{11}C]**1** and [^{11}C]**4** as new potential PET agents for imaging of sEH and PDE4 enzymes in neuroinflammation.

Acknowledgments

This work was partially supported by the Hebei Province Major Science and Technology Program (No. 17392605D), and the High Level Scientific and Technological Innovation and Entrepreneurial Talent Plan of Shijiazhuang in China. This work was also partially supported by the Indiana University Department of Radiology and Imaging Sciences in the United States.

References and notes

1. Heukels P, Moor CC, von der Thüsen JH, Wijsenbeek MS, Kool M. Inflammation and immunity in IPF pathogenesis and treatment. Respir Med. 2019;147:79-91.
2. Knezevic D, Mizrahi R. Molecular imaging of neuroinflammation in Alzheimer’s disease and mild cognitive impairment. Prog Neuropsychopharmacol Biol Psychiatry. 2018;80(Pt B):123-131.
3. Chen WW, Zhang X, Huang WJ. Role of neuroinflammation in neurodegenerative diseases (Review). Mol Med Rep. 2016;13:3391-3396.
4. Kielian T. Neuroinflammation: good, bad, or indifferent? J Neurochem. 2014;130:1-3.
5. Calsolaro V, Edison P. Neuroinflammation in Alzheimer's disease: Current evidence and future directions. Alzheimer’s Dement. 2016;12:719-732.
6. Cerami C, Iaccarino L, Perani D. Molecular imaging of neuroinflammation in neurodegenerative dementias: The role of in vivo PET imaging. Int J Mol Sci. 2017;18: E993.
7. Schain M, Kreisl WC. Neuroinflammation in neurodegenerative disorders-a review. Curr Neurol Neurosci Rep. 2017;17:25.
8. Albrecht DS, Granziera C, Hooker JM, Loggia ML. In vivo imaging of human neuroinflammation. ACS Chem Neurosci. 2016;7:470-483.
9. Gargiulo S, Coda AR, Panico M, Gramanzini M, Moresco RM, Chalon S, Pappatà S. Molecular imaging of neuroinflammation in preclinical rodent models using positron emission tomography. Q J Nucl Med Mol Imaging. 2017;61:60-75.
10. Ory D, Celen S, Verbruggen A, Bormans G. PET radioligands for in vivo visualization of neuroinflammation. Curr Pharm Des. 2014;20:5897-5913.
11. Narayanaswami V, Dahl K, Bernard-Gauthier V, Josephson L, Cumming P, Vasdev N. Emerging PET radiotracers and targets for imaging of neuroinflammation in neurodegenerative diseases: Outlook beyond TSPO. Mol Imaging. 2018;17:1-25.
12. Zheng Q.-H, Fei X, DeGrado TR, Wang JQ, Stone KL, Martinez TD, Gay DJ, Baity WL, Mock BH, Glick-Wilson BE, Sullivan ML, Miller KD, Sledge GW, Hutchins GD. Synthesis, biodistribution and micro-PET imaging of a potential cancer biomarker carbon-11 labeled MMP inhibitor (2*R*)-2-[[4-(6-fluorohex-1-ynyl)phenyl]sulfonylamino]-3-methylbutyric acid [^{11}C]methyl ester. Nucl Med Biol. 2003;30:753-760.
13. Gao M, Wang M, Miller KD, Zheng Q.-H. Synthesis and preliminary in vitro biological evaluation of new carbon-11-labeled celecoxib derivatives as candidate PET tracers for imaging of COX-2 expression in cancer. Eur J Med Chem. 2011;46:4760-4767.
14. Wang M, Yoder KK, Gao M, Mock BH, Xu XM, Saykin AJ, Hutchins GD, Zheng Q.-H. Fully automated synthesis and initial PET evaluation of [^{11}C]PBR28. Bioorg Med Chem Lett. 2009;19:5636-5639.
15. Gao M, Wang M, Miller KD, Hutchins GD, Zheng Q.-H. Synthesis and in vitro biological evaluation of carbon-11-labeled quinoline derivatives as new candidate PET radioligands for cannabinoid CB2 receptor imaging. Bioorg Med Chem. 2010;18:2099-2106.
16. Wang M, Gao M, Miller KD, Sledge GW, Hutchins GD, Zheng Q.-H. The first synthesis of [^{11}C]SB-216763, a new potential PET agent for imaging of glycogen synthase kinase-3 (GSK-3). Bioorg Med Chem Lett. 2011;21:245-249.
17. Gao M, Wang M, Meyer JA, Peters JS, Zarrinmayeh H, Territo PR, Hutchins GD, Zheng Q.-H. Synthesis and preliminary biological evaluation of [^{11}C]methyl (2-amino-5-(benzylthio)thiazolo[4,5-d]pyrimidin-7-yl)-d-leucinate for the fractalkine receptor (CX_3CR1). Bioorg Med Chem Lett. 2017;27:2727-2730.
18. Gao M, Wang M, Green MA, Hutchins GD, Zheng Q.-H. Synthesis of [^{11}C]GSK1482160 as a new PET

agent for targeting $P2X_7$ receptor. Bioorg Med Chem Lett. 2015;25:1965-1970.
19. Territo PR, Meyer JA, Peters JS, Riley AA, McCarthy BP, Gao M, Wang M, Green MA, Zheng Q.-H, Hutchins GD. Characterization of ^{11}C-GSK1482160 for targeting the P2X7 receptor as a biomarker for neuroinflammation. J Nucl Med. 2017;58:458-465.
20. Wang X, Xu W, Miao C, Dong F, Li W, Wang M, Gao M, Zheng Q.-H, Xu Z. Synthesis of *N*-(3-(4-[^{11}C]methylpiperazin-1-yl)-1-(5-methylpyridin-2-yl)-1*H*-pyrazol-5-yl)pyrazolo[1,5-*a*]pyrimidine-3-carboxamide as a new potential PET agent for imaging of IRAK4 enzyme in neuroinflammation. Appl Radiat Isot. 2018;132:6-12.
21. Espinoza-Fonseca LM. The benefits of the multi-target approach in drug design and discovery. Bioorg Med Chem. 2006;14:896-897.
22. Talevi A. Multi-target pharmacology: possibilities and limitations of the "skeleton key approach" from a medicinal chemist perspective. Front Pharmacol. 2015;6:205.
23. Ramsay RR, Popovic-Nikolic MR, Nikolic K, Uliassi E, Bolognesi ML. A perspective on multi-target drug discovery and design for complex diseases. Clin Transl Med. 2018;7:3.
24. Reddy AS, Zhang S. Polypharmacology: drug discovery for the future. Expert Rev Clin Pharmacol. 2013;6:41-7.
25. Blöcher R, Wagner KM, Gopireddy RR, Harris TR, Wu H, Barnych B, Hwang SH, Xiang YK, Proschak E, Morisseau C, Hammock BD. Orally available soluble epoxide hydrolase/phosphodiesterase 4 dual inhibitor treats inflammatory pain. J Med Chem. 2018;61:3541-3550.
26. Ibrahim MM, Gabr MT. Multitarget therapeutic strategies for Alzheimer's disease. Neural Regen Res. 2019;14:437-440.
27. Kenk M, Thomas A, Lortie M, Dekemp R, Beanlands RS, Dasilva JN. PET measurements of cAMP-mediated phosphodiesterase-4 with (*R*)-[^{11}C]rolipram. Curr Radiopharm. 2011;4:44-58.
28. Horti AG, Wang Y, Minn I, Lan X, Wang J, Koehler RC, Alkayed NJ, Dannals RF, Pomper MG. ^{18}F-FNDP for PET imaging of soluble epoxide hydrolase. J Nucl Med. 2016;57:1817-1822.
29. Souness JE, Griffin M, Maslen C, Ebsworth K, Scott LC, Pollock K, Palfreyman MN, Karlsson JA. Evidence that cyclic AMP phosphodiesterase inhibitors suppress TNF alpha generation from human monocytes by interacting with a 'low-affinity' phosphodiesterase 4 conformer. Br J Pharmacol. 1996;118:649-658.
30. Blöcher R, Lamers C, Wittmann SK, Merk D, Hartmann M, Weizel L, Diehl O, Brüggerhoff A, Boß M, Kaiser A, Schader T, Göbel T, Grundmann M, Angioni C, Heering J, Geisslinger G, Wurglics M, Kostenis E, Brüne B, Steinhilber D, Schubert-Zsilavecz M, Kahnt AS, Proschak E. *N*-Benzylbenzamides: A novel merged scaffold for orally available dual soluble epoxide hydrolase/peroxisome proliferator-activated receptor gamma modulators. J Med Chem. 2016;59:61-81.
31. Jiang L, Yu J, Niu F, Zhang D, Sun X. A high-efficient method for the amidation of carboxylic acids promoted by triphenylphosphine oxide and oxalyl chloride. Heteroatom Chem. 2017;28:e21364.
32. Aiello F, Shabaik Y, Esqueda A, Sanchez TW, Grande F, Garofalo A, Neamati N. Design and synthesis of 3-carbamoylbenzoic acid derivatives as inhibitors of human apurinic/apyrimidinic endonuclease 1 (APE1). ChemMedChem. 2012;7:1825-1839.
33. Yan YL, Miller MT, Cao Y, Cohen SM. Synthesis of hydroxypyrone- and hydroxythiopyrone-based matrix metalloproteinase inhibitors: developing a structure-activity relationship. Bioorg Med Chem Lett. 2009;19:1970-1976.
34. Zhao Z, Pissarnitski DA, Josien HB, Bara TA, Clader JW, Li H, McBriar MD, Rajagopalan M, Xu R, Terracina G, Hyde L, Song L, Zhang L, Parker EM, Osterman R, Buevich AV. Substituted 4-morpholine *N*-arylsulfonamides as γ-secretase inhibitors. Eur J Med Chem. 2016;124:36-48.
35. Gao M, Wang M, Zheng Q.-H. Synthesis of carbon-11-labeled CK1 inhibitors as new potential PET radiotracers for imaging of Alzheimer's disease. Bioorg Med Chem Lett. 2018;28:2234-2238.
36. Jewett DM. A simple synthesis of [^{11}C]methyl triflate. Int J Rad Appl Instrum A. 1992;43:1383-1385.
37. Mock BH, Mulholland GK, Vavrek MT. Convenient gas phase bromination of [^{11}C]methane and production of [^{11}C]methyl triflate. Nucl Med Biol. 1999;26:467-471.
38. Wang M, Gao M, Zheng Q.-H. Fully automated synthesis of PET TSPO radioligands [^{11}C]DAA1106 and [^{18}F]FEDAA1106. Appl Radiat Isot. 2012;70:965-973.
39. Mock BH, Zheng Q.-H, DeGrado TR. A multi-purpose ^{11}C-radio-synthesis system. J Labelled Compd Radiopharm. 2005;48:S225.
40. Mock BH, Glick-Wilson BE, Zheng Q.-H, DeGrado TR. Automated measurement of specific activity of radiolabeled ligands during synthesis. J Labelled Compd Radiopharm. 2005;48:S224.
41. Zheng Q.-H, Mock BH. Purification of carbon-11 PET radiotracers from unlabeled precursors by preparative HPLC and SPE. Biomed Chromatogr. 2005;19:671-676.
42. *(a). General:* All commercial reagents and solvents were purchased from Sigma-Aldrich and Fisher Scientific, and used without further purification. [^{11}C]CH_3OTf was prepared according to a literature procedure.[37] Melting points were determined on WRR apparatus and were uncorrected. ^{1}H and ^{13}C NMR spectra were recorded on a Bruker Avance II 600 or 400 MHz NMR Fourier transform spectrometer at 600 or 100 MHz, respectively. Chemical shifts (δ) are reported in parts per million (ppm) relative to an internal standard tetramethylsilane (TMS, δ 0.0) (^{1}H

NMR) and to the solvent signal (^{13}C NMR), and coupling constants (*J*) are reported in hertz (Hz). Liquid chromatography-mass spectra (LC-MS) analysis was performed on AB Sciex 4000Q Trap instrument, consisting of an 1100 series HPLC connected to a diode array detector and a 1946D mass spectrometer configured for positive-ion/negative-ion electrospray ionization (ESI). The high resolution mass spectra (HRMS) were obtained using a Waters/Micromass LCT Classic spectrometer. Chromatographic solvent proportions are indicated as volume : volume ratio. Thin-layer chromatography (TLC) was run using HS silica gel GF254 uniplates (5 × 10 cm^2). Plates were visualized under UV light. Normal phase flash column chromatography was carried out on Combiflash Rf 150 silica gel 60 (300-400 mesh) with a forced flow of the indicated solvent system in the proportions described below. All moisture- and air-sensitive reactions were performed under a positive pressure of nitrogen maintained by a direct line from a nitrogen source. Analytical RP-HPLC was performed using a Prodigy (Phenomenex) 5 μm C-18 column, 4.6 × 250 mm; mobile phase 65% CH_3CN/35% 4.0 mM CH_3COONa; flow rate 1.0 mL/min; UV (254 nm) and γ-ray (PIN diode) flow detectors. Semi-preparative RP-HPLC column was performed using a Prodigy (Phenomenex) 5 μm C-18 column, 10 × 250 mm; 70% CH_3CN/30% H_2O mobile phase; 5 and 4 mL/min flow rate for [^{11}C]**1** and [^{11}C]**4**, respectively; UV (254 nm) and γ-ray (PIN diode) flow detectors. C18 Plus Sep-Pak cartridges were obtained from Waters Corporation (Milford, MA). Sterile Millex-FG 0.2 μm filter units were obtained from Millipore Corporation (Bedford, MA).

*(b). N-(4-Methoxy-2-(trifluoromethyl)benzyl)benzamide (**1**):* To a stirred solution of benzoic acid (0.2 g, 0.85 mmol) in dichloromethane (CH_2Cl_2, 10 mL), EDC (320 mg, 2.00 mmol), and DMAP (40 mg, 0.34 mmol) were added at room temperature (RT) under a nitrogen atmosphere. After the reaction was continued for 1 h, (4-methoxy-2-(trifluoromethyl)phenyl)methanamine (160 μL, 0.93 mmol) was added, and the reaction was continued at RT for another 24 h. Water (30 mL) was added to the reaction mixture, and then the resulted solution was extracted with CH_2Cl_2 (3 × 30 mL). The combined organic layer was washed with 1 N NaOH (3 × 20 mL), 1 N HCl (3 × 20 mL) and brine (3 × 20 mL), dried over anhydrous Na_2SO_4 and filtered. The solvent was evaporated under vacuum. The resulted crude product was purified by silica gel column chromatography with petroleum ether (PE)/EtOAc (3:1) as eluent to afford **1** as a white solid (0.22 g, 84%), mp 106.3-110.7 ºC. ^1H NMR (600 MHz, $CDCl_3$): δ 7.75 (d, *J* = 7.7 Hz, 2H), 7.57 (d, *J* = 8.5 Hz, 1H), 7.49 (t, *J* = 7.3 Hz, 1H), 7.42 (t, *J* = 7.6 Hz, 2H), 7.18 (d, *J* = 2.2 Hz, 1H), 7.03 (dd, *J* = 8.4, 1.9 Hz, 1H), 6.48 (s, 1H), 4.74 (d, *J* = 5.9 Hz, 2H), 3.83 (s, 3H). (LC-MS, *m/z*): Calcd for $C_{16}H_{15}F_3NO_2$ ([M+H]$^+$) 310.1, found:310.1.

*(c). N-(4-Hydroxy-2-(trifluoromethyl)benzyl)benzamide (**2**):* To a stirred solution of **1** (27 mg, 0.086 mmol) in CH_2Cl_2 (5 mL), BBr_3 (50 μL, 0.52 mmol) was added slowly at 0 ºC, the reaction mixture was warmed up to RT and continued for 20 h. The reaction mixture was poured into ice water (10 mL), and then the CH_2Cl_2 was removed under reduced pressure. The resulted aqueous solution was extracted with EtOAc (3 × 20 mL). The combined organic layer was washed with water, brine, dried over anhydrous Na_2SO_4 and filtered. The organic solution was evaporated under vacuum, and the resulted product was purified by silica gel column chromatography with PE/EtOAc (1:1) as eluent to afford **2** as a white solid (15 mg, 59%), mp 122.5-124 ºC. ^1H NMR (600 MHz, $CDCl_3$): δ 9.97 (s, 1H), 8.96 (t, *J* = 5.4 Hz, 1H), 7.90 (d, *J* = 7.3 Hz, 2H), 7.55 (t, *J* = 7.3 Hz, 1H), 7.48 (t, *J* = 8.5 Hz, 2H), 7.33 (d, *J* = 8.5 Hz, 1H), 7.07 (d, *J* = 2.2 Hz, 1H), 7.01 (dd , *J* = 8.4, 1.7 Hz, 1H), 4.54 (d, *J* = 5.4 Hz, 2H). ^{13}C NMR (100MHz, MeOD): δ 169.28, 157.10, 155.44, 143.56, 134.01, 131.51, 130.53, 128.21 (2C), 127.11, 118.42, 116.58, 115.18, 112.56, 40.73. HRMS (ESI, *m/z*): Calcd for $C_{15}H_{13}F_3NO_2$ ([M+H]$^+$) 296.0893, found: 296.0887.

*(d). Propionylpiperidine-4-carboxylic acid (**3**):* To a stirred solution of methyl 4-piperidinecarboxylate (4.5 g, 30 mmol) in CH_2Cl_2 (10 mL), propionyl chloride (3.5 mL, 40 mmol) and triethyl amine (5.6 mL, 37 mmol) were added slowly at 0 ºC. The reaction was continued at 0 ºC for 4 h. Then the reaction was quenched by adding water (10 mL), and extracted with CH_2Cl_2 (2 × 20 mL). The combined organic layer was washed with water, brine, dried over anhydrous Na_2SO_4 and filtered. After the solvent was removed under reduced pressure, methanol (20 mL) and aqueous NaOH (5.0 N, 20 mL) were added to the residue. The resulted mixture was stirred at RT for 16 h. The methanol was removed under reduced pressure, and pH of the solution was adjusted to 6-7 with 5 N aqueous HCl. The mixture was extracted with CH_2Cl_2 (3 × 50 mL), and the combined organic layer was washed with water, brine, dried over anhydrous Na_2SO_4 and filtered. The solvent was evaporated under vacuum, and the crude product was purified by silica gel column chromatography with PE/EtOAc (3:1) as eluent to afford **3** as a white solid (5.11 g, 88%), mp 86.5-87.8 ºC. ^1H NMR (600MHz , $CDCl_3$): δ 4.41 (d, *J* = 13.3 Hz, 1H), 3.82 (d, *J* = 13.6 Hz, 1H), 3.16 - 3.11 (m, 1H) , 2.88 - 2.83 (m, 1H) , 2.60 - 2.56 (m, 1H), 2.39 - 2.35 (m, 2H), 1.98 - 1.96 (m, 2H), 1.74 - 1.63 (q, *J* = 7.4 Hz, 2H), 1.15 (t, *J* = 7.4 Hz, 3H). (LC-MS, *m/z*): Calcd for $C_9H_{16}NO_3$ ([M+H]$^+$) 186.2, found:186.4

*(e). N-(4-Methoxy-2-(trifluoromethyl)benzyl)-1-propionylpiperidine-4-carboxamide (MPPA, **4**):* Compound **4** was prepared by following the synthesis

procedure of compound **1**. The crude product was purified by silica gel column chromatography with CH_2Cl_2/CH_3OH (10:1) as eluent to afford **4** as a white solid (0.26 g, 70%), mp 132.4-136.9 ºC. ^1H NMR (600 MHz, $CDCl_3$): δ 7.45 (d, J = 8.5 Hz, 1H), 7.16 (d, J = 2.6 Hz, 1H), 7.02 (dd, J = 8.5, 2.6 Hz, 1H), 5.81 (s, 1H), 4.53 (d, J = 5.6 Hz, 2H), 3.83 (s, 3H), 3.05 - 3.00 (m, 1H), 2.65 - 2.00 (m, 1H), 2.35 - 2.28 (m, 3H), 1.91 - 1.81 (m, 2H), 1.70 - 1.57 (m, 4H), 1.13 (t, J = 7.4, 3H). (LC-MS, *m/z*): Calcd for $C_{18}H_{24}F_3N_2O_3$ ($[M+H]^+$) 373.4, found: 373.2

*(f). N-(4-Hydroxy-2-(trifluoromethyl)benzyl)-1-propionylpiperidine-4carboxamide (**5**):* Compound **5** was prepared by following the synthesis procedure of compound **2**. The crude product was purified by silica gel column chromatography with CH_2Cl_2/CH_3OH (8:1) as eluent to afford **5** as a white solid (17 mg, 55%), mp 142.5-145.3 ºC. ^1H NMR (600 MHz, DMSO-d6): δ 8.29 (t, J = 5.5 Hz, 1H), 7.23 (d, J = 8.5 Hz, 1H), 7.03 (d, J = 2.2 Hz, 1H), 6.98 (dd, J = 8.5, 1.7 Hz, 1H), 4.29 (d, J = 5.2 Hz, 2H), 3.86 (d, J = 13.5Hz, 1H), 2.98 (t, J =12.3 Hz, 1H), 2.54 (t, J = 11.4 Hz, 1H), 2.47 - 2.42 (m, 1H), 2.34 - 2.25 (m, 2H), 1.72 (t, J = 14.6Hz, 2H), 1.53 - 1.23 (m, 2H), 0.97 (t, J = 7.4 Hz, 3H). ^{13}C NMR (100 MHz, MeOD): δ 175.63, 173.32, 156.78, 131.22, 126.49, 124.38, 118.44, 118.16, 112.46, 44.89, 42.37, 41.08, 39.11, 28.79, 28.21, 25.88, 8.59. HRMS (ESI, *m/z*): Calcd for $C_{17}H_{22}F_3N_2O_3$ ($[M+H]^+$) 359.1577, found: 359.1569.

*(g). N-(4-[^{11}C]methoxy-2-(trifluoromethyl)benzyl)benzamide ([^{11}C]**1**) and N-(4-[^{11}C]methoxy-2-(trifluoromethyl)benzyl)-1-propionylpiperidine-4-carboxamide ([^{11}C]MPPA, [^{11}C]**4**):* [^{11}C]CO_2 was produced by the $^{14}N(p,\alpha)^{11}C$ nuclear reaction in the small volume (9.5 cm^3) aluminum gas target provided with the Siemens RDS-111 Eclipse cyclotron. The target gas consisted of 1% oxygen in nitrogen purchased as a specialty gas from Praxair, Indianapolis, IN. Typical irradiations used for the development were 58 µA beam current and 20 min on target. The production run produced approximately 37.0 GBq of [^{11}C]CO_2 at EOB. The precursor **2** or **5** (0.1-0.3 mg) was dissolved in CH_3CN (500 µL). To this solution was added aqueous NaOH (2 N, 2 µL). The mixture was transferred to a small reaction vial. No-carrier-added (high molar activity) [^{11}C]CH_3OTf that was produced by the gas-phase production method[37] within 12 min from [^{11}C]CO_2 through [^{11}C]CH_4 and [^{11}C]CH_3Br with AgOTf column was passed into the reaction vial at RT until radioactivity reached a maximum (2 min), and then the reaction vial was isolated and heated at 80 °C for 3 min. The contents of the reaction vial were diluted with aqueous $NaHCO_3$ (0.1 M, 1 mL). The reaction vial was connected to a 3-mL HPLC injection loop. The labeled product mixture solution was injected onto the semi-preparative HPLC column for purification. The product fraction was collected in a recovery vial containing 30 mL water. The diluted tracer solution was then passed through a C-18 Plus Sep-Pak cartridge, and washed with water (3 × 10 mL). The cartridge was eluted with EtOH (3 × 0.4 mL) to release the labeled product, followed by saline (10-11 mL). The eluted product was then sterile-filtered through a Millex-FG 0.2 µm membrane into a sterile vial. Total radioactivity was assayed and total volume (10-11 mL) was noted for tracer dose dispensing. The overall synthesis time including HPLC-SPE purification and reformulation was 35-40 min from EOB. The decay corrected radiochemical yield was 25-35%. Retention times in the analytical RP-HPLC system were: t_R **2** = 3.57 min, t_R **1** = 6.56 min, and t_R [^{11}C]**1** = 6.64 min; and t_R **5** = 2.76 min, t_R **4** = 4.23 min, and t_R [^{11}C]**4** = 4.31 min. Retention times in the preparative RP-HPLC system were: t_R **2** = 5.25 min, t_R **1** = 7.67 min, and t_R [^{11}C]**1** = 7.74 min; and t_R **5** = 4.52 min, t_R **4** = 6.78 min, and t_R [^{11}C]**4** = 6.83 min.